Inter-Research Science Publisher

Marine Ecology Progress Series
Volume 755:63–77

Published February 27, 2025
https://doi.org/10.3354/meps14795

Anaerobic decomposition dynamics of three kelp species from the North-east Atlantic: implications for blue carbon storage

A. R. O'Dell[1,*], J. M. Baxter[2], P. J. Moore[3], D. A. Smale[4], C. Smeaton[5], I. M. Davies[6], M. T. Burrows[1]

[1]Scottish Association for Marine Science (SAMS), Oban PA37 1QA, UK
[2]School of Biology, University of St Andrews, St Andrews KY16 8LB, UK
[3]Dove Marine Laboratory, School of Natural and Environmental Sciences, Newcastle University, Newcastle-upon-Tyne NE1 7RU, UK
[4]Marine Biological Association of the United Kingdom, Citadel Hill, Plymouth PL1 2PB, UK
[5]School of Geography and Sustainable Development, University of St Andrews, St Andrews KY16 9AL, UK
[6]Marine Directorate, Scottish Government, 375 Victoria Road, Aberdeen AB11 9DB, UK

ABSTRACT: Decomposition pathways of detritus are key processes in the contribution of macroalgal habitats to natural carbon sequestration of 'blue carbon'. The anaerobic decomposition of 3 North-east Atlantic canopy-forming kelp species was investigated using *ex situ* decomposition chambers. Thallus parts (stipes, holdfasts and blades) of *Laminaria hyperborea, Saccharina latissima* and *L. digitata* were incubated in still seawater in temperature-controlled dark conditions. Refractory potential (Rp), first-order decomposition rate (k) and associated half-life ($t_{1/2}$) were calculated. Dissolved organic and inorganic carbon (DOC and DIC, respectively) were measured in the incubation water at 0, 7, 14 and 21 d, and thermal gravimetric profiles were determined at each decomposition stage. Oxygen depletion occurred within 24 h. Approximately 5 times as much DOC was released than DIC. Holdfast material produced the most DIC, while blade material released the greatest amounts of DOC. *S. latissima* released less DOC than *L. hyperborea* and *L. digitata*. The mean (SD) Rp of fragments increased from 0.46 ± 0.05 to 0.50 ± 0.04 throughout the 21 d incubations. *S. latissima* had the highest Rp throughout. First-order decomposition rates, averaged across the 3 kelp species, gave half-lives ($t_{1/2}$) for blade fragments of 27.8 ± 2.9 d, (k = 0.025 ± 0.002) and stipes as 113.2 ± 21.1 d (k = 0.006 ± 0.001). This experiment clarifies the fate of macroalgal carbon during early decomposition and thus the processes that govern blue carbon pathways of macroalgae, highlighting the differences in breakdown among different species and thallus parts.

KEY WORDS: Macroalgae · Kelp · Carbon · Decomposition · Blue carbon

1. INTRODUCTION

Blue carbon habitats, such as salt marsh, mangroves and seagrass meadows, play a central role in fixing, storing and exporting carbon in coastal ecosystems, and their potential to mitigate increasing anthropogenic atmospheric carbon dioxide has led to increased research effort and wider interest in the field (Mcleod et al. 2011, Pendleton et al. 2012, Macreadie et al. 2017, 2019, Hori et al. 2019). However, understanding the pathways of carbon storage among blue carbon habitats and wider ecosystems is not straightforward, as the processes involved are difficult to quantify. Macroalgal habitats, for example, are not considered to be carbon sinks, but instead contribute to carbon storage pathways via the production and

*Corresponding author: alasdair.odell@sams.ac.uk

export of significant amounts of detritus and dissolved organic carbon (DOC) (Krumhansl & Scheibling 2011, 2012, Krause-Jensen & Duarte 2016, Smale et al. 2022). Quantifying the contribution of macroalgal detritus to long-term carbon stores depends upon the measurement of processes that occur in unknown locations or at depths that are not easily accessible. For example, pulses of detritus have been observed accumulating in shallow sediments and into deeper benthic zones (400 m plus) in fjords in the North-east Atlantic (Filbee-Dexter et al. 2018). Macroalgal detritus has even been found contributing to sediments as far as 5000 km from shore and at depths of over 4000 m, likely from floating rafts that eventually sink (Ortega et al. 2019).

Subsidies of detritus from macroalgal habitats are ubiquitous and important resources, both in benthic environments (Smale et al. 2022) and as beach-cast deposits which will decompose in a more terrestrial environment (Gilson et al. 2021). However, these subsidies are often transient and can be transported in pulses from coastal areas into the shallow inshore subtidal (12–85 m), deeper fjords (400–450 m) and canyons (700–900 m), and into the deep ocean where material may accumulate (Vetter & Dayton 1999, Filbee-Dexter et al. 2018, 2024). The timing, quantity and persistence of detritus within recipient habitats has a strong influence on the structure and functioning of associated macrofaunal communities (Ehrnsten et al. 2019, Queirós et al. 2019, de Bettignies et al. 2020). Furthermore, accumulations of macroalgae will influence the local sediment geochemistry, often creating anoxic conditions, as microbes (including bacteria and fungi) rapidly colonise the material and consume oxygen through their metabolism (Green-Cavrielidis et al. 2018, Perkins et al. 2021, 2023). Through consumption of organic matter, the fixed carbon within macroalgal tissues can be released in 2 main forms. Firstly, particulate carbon forms as material weakens and pieces break off. Secondly, the dissolved forms of carbon originate from multiple pathways. DOC usually originates from exudation of cellular material and occasionally from microbial respiration, and dissolved inorganic carbon (DIC) is usually a biproduct of respiration. DIC can be in the form of carbonates, bicarbonates or CO_2 (Dafner & Wangersky 2002, Jiao et al. 2010).

The breakdown of organic material is controlled by multiple factors, with the process usually expressed in terms of first-order decomposition by the rate constant k for the single-pool negative exponential model of litter mass-loss during decomposition (Olson 1963, Enríquez et al. 1993, Laliberté et al. 2012). In the marine environment, the strongest influences on rates of breakdown are oxygen availability, temperature and the biochemical composition of litter (Filbee-Dexter et al. 2022). Temperature is considered a driving factor in aerobic decomposition, although it has been shown to have less of an impact on anaerobic microbial activity (Zhang et al. 2008). Macroalgae lack the structural lignocellulose matrix common in terrestrial plants (Burton et al. 2010). Instead, cell walls of brown algae are composed of polymeric alginates and fucose-containing sulphated polysaccharides (or fucoidans) which interlock β-glucan scaffolds that are rich in cellulose. However, the composition of cell walls varies among macroalgal species and can include alginates, xylans, carrageenans, agars, fucoidans and mannans as well as more complex compounds such as proteins (Deniaud-Bouët et al. 2017). This highly variable composition of cell walls means that rates of decomposition and the decomposition products of macroalgal material can differ significantly between algal species (Trevathan-Tackett et al. 2015).

Litter quality refers to the chemical composition of a resource and often indicates its availability to decomposing organisms. It is commonly expressed by the nitrogen content (N), C:N ratio, lignin content and the ratio of nitrogen to lignin (Gholz et al. 2000, Prescott et al. 2000, Zhang et al. 2008). The proportion of biopolymers such as lignin in detritus is important in organic matter breakdown (Meentemeyer 1978). Lignin is present in blue carbon systems such as seagrass and mangroves (Ola & Lovelock 2021). Macroalgae lack lignin but can be rich in phlorotannins, polymers of phloroglucinol, and structural compounds such as cellulose, which due to their multiple aromatic carbon rings and complex structures will influence the quality of macroalgal detritus (Haavisto et al. 2017). The composition of macroalgal material differs seasonally with known storage compounds (such as laminarin) present in greater amounts after productive summer months (Schiener et al. 2015). Moreover, different components of complex canopy-forming macroalgae (such as kelps and fucoids) serve different functions and therefore have different tissue types. For example, holdfast material firmly grips hard substrates and is known to produce bio-adhesives (Kerrison et al. 2019), stipe material provides rigidity in some species and flexibility in others to compensate for wave-action and laminar flow in differing energetic environments (Johnson & Koehl 1994), and blade material has high surface area for gaseous exchange with seawater and increased pho-

tosynthesis. As such, it is highly likely that the different biochemical composition of different tissue types will lead to different decay rates, yet this has rarely been examined.

Recent publications have demonstrated that macroalgae contribute to sedimentary carbon sinks and that this previously overlooked blue carbon habitat plays a role as a donor for wider carbon storage (Filbee-Dexter et al. 2018, Krause-Jensen et al. 2018, Queirós et al. 2019, Filbee-Dexter & Wernberg 2020, Pedersen et al. 2021). The decomposition dynamics of macroalgal detritus plays an important role in the cycling of fixed carbon. However, little is known about the dynamics of carbon remineralisation and sequestration within accumulations of detritus, particularly in areas below the photic zone. By comparing rates of decomposition of kelp material in anaerobic chambers, the following hypotheses were addressed: (1) different kelp species and different tissue types will decompose at different rates according to the differences in their biochemical composition and linked to their morphology (for example, more rigid, structural material in *Laminaria hyperborea*); (2) microbial activity will rapidly break down macroalgal detritus, releasing CO_2 at high rates into the surrounding seawater; and (3) detrital material will become more refractory over time as labile compounds are consumed first, leaving more complex compounds behind. The present study aims to address these unknowns and build upon existing data (see Pedersen et al. 2021) by comparing decomposition across the different parts of the thallus, which can reduce the uncertainty around important decomposition metrics (i.e. *k*). Moreover, understanding the loss (remineralisation) or retention of the organic carbon within detritus-producing, macroalgal species will help clarify the contribution that the habitats formed by macroalgae play within blue carbon frameworks.

2. MATERIALS AND METHODS

2.1. Species selection and field sampling

Twelve custom-made incubation tubes were used in this experiment; the tubes were 300 mm long with a 60 mm diameter (560 ml volume). Each end was fitted with a lid and a rubber O-ring to allow airtight seals, and both ends were fitted with a Luer lock fitting to allow air to be pushed through and removed entirely (full schematic, Fig. S1 in Section S1 in the Supplement at www.int-res.com/articles/suppl/m755p063_supp.pdf). *Saccharina latissima*, *Laminaria hyperborea* and *L. digitata* were chosen as they are dominant, canopy-forming species responsible for much of the production of detritus in the North-east Atlantic (Walker 1954). Samples were randomly collected from 9 different locations in Argyll, Scotland, from February 2019 to July 2020 (a fresh sampling event for each incubation run). All kelp samples were processed within 4 h of collection; to mirror real-world detritus, no epiphytes were removed. The blades, holdfasts and stipes of each species were cut into equal sized fragments: 25 × 10 cm for blades, 25 cm length for stipes, and holdfasts used whole or trimmed to fit in the tube (diameter 6 cm). While the size of the fragments was controlled, biomass varied between species and tissues (approximate blade weights were between 20 and 35 g, stipes were heavier and varied between 30 and 200 g, holdfasts were between 10 and 50 g), so each fragment was weighed individually (see dry mass calculations at the end of this paragraph). The fragments were then randomly allocated to separate tubes for incubations (n = 14) in 21 d runs of batches of 10 tubes. Incubations of 7, 14 and 21 d were performed in the dark in a temperature-controlled room (11−13°C, to match local mean surface seawater temperatures in spring/summer) in filtered seawater. Seawater was taken from Dunstaffnage Bay, Oban, and filtered through a Lacron sand (0.45−0.55 mm) filter to 20−40 µm to remove phytoplankton and other multicellular organisms but not marine microbes. Four replicates of stipe, blade and holdfast material from the 3 kelp species were incubated for each incubation period (7, 14, 21 d). All tubes were stored horizontally to reduce oxygen stratification, but since oxygen was found to deplete rapidly (within 24 h), no agitation was applied to reduce oxygen stratification. Two control tubes containing seawater only were run with each batch of incubations to be sampled at each sampling point. At each sampling point, tube water and contents were sacrificed. A sample from each replicate was taken before experimentation to establish initial carbon content of the individual plants and tissue types. Each sample was oven dried (60°C, 48 h), homogenised using a high-powered blender and dry mass was calculated. Approximately 10 mg were weighed into silver capsules for C and N analysis, and the rest was kept for subsequent analysis (see Section S2).

Oxygen was measured using a fibre-optic oxygen meter (FirestingO_2 ®, Pyroscience), following the methods of Mills et al. (2018). Green sensor spots were positioned on a minimum of 2 tubes for each incubation run until all sample types were represented, including control tubes, and sensor readings were

taken every 30 s until oxygen was completely depleted, with the exception of control tubes, which retained oxygen throughout.

2.2. Carbon

2.2.1 Total carbon in macroalgal fragments

Carbon content was calculated following Smeaton & Austin (2019) and Smeaton et al. (2020). Briefly, a random subset (n = 26) of oven-dried (60°C, 48 h) samples, taken from every duration of incubation and including fresh fragments (n = 8) was analysed. To remove carbonates, samples were placed in a desiccator with 37% HCl for 48 h. Samples were further dried for 24 h at 40°C, and organic carbon and nitrogen were measured using an Elementar Vario EL elemental analyser (EA). Triplicate samples were combusted at high temperatures (1200°C), with the evolved gases being measured using thermal conductivity detection. Quality control was assured with repeated analysis of reference material B2178 (Medium Organic Content standard from Elemental Microanalysis) (Smeaton & Austin 2019).

2.2.2. Dissolved inorganic carbon

Incubation tubes were fitted with a Luer lock at each end to allow the tubes to be opened at both ends for extraction of water for DIC determination. DIC collection, treatment protocols and sampling and storage methods followed those developed by Dickson et al. (2007) and Bockmon & Dickson (2015). Opening the tubes at each end allowed water to be removed from the tube without introducing oxygen and CO_2 to the sample. Tube water (100 ml) was extracted into pre-labelled 125 ml borosilicate glass bottles, water was carefully poured down the side of each glass bottle to prevent bubbles forming, and samples were poisoned with 50 µl of (0.05% solution) mercuric chloride ($HgCl_2$) to prevent further production of CO_2 during storage (Dickson et al. 2007). The samples were sealed and stored at 5°C until analysis.

Acidification followed by coulometric quantification has been shown to be highly accurate for DIC estimation (Goyet & Snover 1993). DIC analysis was therefore done using an acidification module attached to a coulometry module (UIC®). Samples were injected into a strong acid, which converts all inorganic carbon into gaseous CO_2. The CO_2 was carried via a carrier gas (N_2) which was bubbled through the system to a coulometry module which contained a light reader and solutions which change colour on contact with CO_2. DIC instrument performance was evaluated twice daily using in-house standards collected from Loch Leven in 2007 and an international DIC standard (Dickson 2019). All reported readings were blank-corrected, and samples were analysed in triplicate.

2.2.3. Dissolved organic carbon

The sampling and analytical protocol for DOC analysis followed the methods of Davidson et al. (2013). All materials used in DOC sampling were acid-washed for a minimum of 24 h in 10% hydrochloric acid (HCl) and oven-combusted for a minimum of 12 h at 400°C. DOC samples were extracted by hand, using glass syringes (50 ml) and hand pushed through a 0.7 µm, pre-combusted (6 h, 450°C) glass fibre filter while wearing polyethylene gloves. Approximately 20 ml of tube water were filtered into a pre-combusted 25 ml glass bottle and preserved with 50 µl 85% orthophosphoric acid (H_3PO_4, to acidify to a pH < 3) and stored at 5°C in the dark until analysis.

DOC analyses used a total organic carbon analyser (Shimadzu® TOC-VCPH) with platinum catalyst (0.5% alumina), with zero-air as the carrier gas reference condition following the methods of Davidson et al. (2013). This instrument was coupled to a non-dispersive infra-red detector, which detected the concentration of CO_2. Before analysis, inorganic carbon was removed from the acidified samples by sparging with carrier gas for 5 min. At the beginning of each day, the machine was 4-point calibrated with a mix of glycine ($C_2H_5NO_2$, Shimadzu ®) and potassium hydrogen phthalate ($C_8H_5KO_4$, Shimadzu ®), giving a stock solution of 1300 µM C and 285 µM N.

2.3. Thermogravimetric analysis (TGA)

While some of the macroalgal material was analysed for carbon, the remaining dried, ground samples were weighed separately (25 mg ± 1 µg) into a 70 µl aluminium oxide crucible and placed in a thermogravimetric analyser (Mettler-Toledo, TGA2) to be heated in a furnace under a constant flow of an inert gas, here N_2, at 20 ml min^{-1}. The ramping profile used was 40–1000°C at a rate of 10°C min^{-1} (Smeaton & Austin 2022). Pure analytical grade standards of known kelp sugars were analysed under the same parameters to compare with kelp detritus TGA curves

and analyse the mass loss of specific compounds. Sugars selected were: 3-phenyl phenol, phloroglucinol (the structural component of phlorotannins), laminarin, D-mannitol, cellulose, alginic acid and D-mannose.

2.4. Data analysis

Most data analyses were performed within R version 4.1.3 (R Core Team 2022). Carbon concentrations in seawater (mg C g^{-1} DOC and DIC, see Section S3) were square-root transformed to better meet normality assumptions and analysed as separate response variables. The effects of days incubated (fixed effect, 4 levels: 0, 7, 14, 21 d), species (fixed effect, 3 levels: *L. hyperborea, S. latissima, L. digitata*) and material (fixed effect, 3 levels: blade, holdfast, stipe) were tested with a generalised linear model for DOC (GLM1) and DIC (GLM2). The shape of the data distribution (non-linear, positively skewed) was incorporated and found to best fit the Gamma (log link) family for both DOC and DIC data through plotting residuals vs. fitted values and distribution normality with a Q-Q plot. Probabilities associated with fixed factors in the GLM were obtained from likelihood ratio tests. Differences in total carbon in decomposing kelp tissues were tested with an ANCOVA in base R to understand the effect of decomposition on the carbon content across the different species (ANCOVA1).

Data from the TGA were extracted (StarEvolution® Mettler-Toledo) and normalised to input mass. Before extraction, all TGA curves were transformed to the first-order derivative to give rates of mass loss as a function of temperature and emphasise temperatures where mass loss was greatest. Previous studies have shown differences in temperature intervals (TIs) that reflect the various labile, refractory and recalcitrant compounds that combust at increasing temperatures during thermal gravimetric analysis (Table S1, Section S4). For the present study, the methods of Trevathan-Tackett et al. (2015) were applied, giving TIs of: TI 1, 160–300°C for proteins, soluble carbohydrates and hemicellulose; TI 2, 301–400°C for insoluble polysaccharides and compounds such as cellulose and lipids; and TI 3, 401–600°C for insoluble polysaccharide residues and lignin-like compounds. The final TI, TI 4 (601–800°C), categorises the loss of residual organics and inorganics (beyond 800°C, little mass change was observed). Subsequently, the amount of mass lost at the 4 TIs (TIs 1–4) was analysed with a multifactorial permutational analysis of variance (PERMANOVA 1). The TI matrix was plotted as a non-metric multidimensional scaling (NMDS) plot derived from a Bray-Curtis similarity matrix.

The percentages of mass lost at different TIs (Table S2 in Section S5) in matrix form were square-root transformed and the effects of the different categorical groups of days incubated (factor: 4 levels: 0, 7, 14, 21 d), material (factor: 3 levels: blade, stipe and holdfast) and species (factor, 3 levels: *L. hyperborea, S. latissima, L. digitata*) were tested. NMDS and PERMANOVA were done using the 'vegan' package in R (Oksanen et al. 2020).

The refractory potential (Rp) index defined by Kristensen (1990) was applied to the mass lost at TIs 1 & 2 (full methods in Section S6) to show the differences in the refractory nature of compounds within the material at the different time intervals. Decomposition is generally expressed as a first-order rate process. Here, the dry mass of macroalgae material was treated as the reactant to calculate decay over time during this experiment since carbon content was found to be a constant proportion of dry mass (Sections S7 & S8, Fig. S2). The resulting Rp values were tested for significant differences using a 3-way ANOVA to compare the effect of time, species and tissue on the Rp (independent variable).

3. RESULTS

3.1. Dissolved oxygen and total carbon in kelp tissues

Oxygen depletion occurred within 24 h, suggesting that microbe communities rapidly remineralise compounds in the water column and kelp tissues. The mean ± SD total carbon content was 23.4 ± 2.7% (Section S8, Fig. S2), and there was no significant difference in total organic carbon content, even when testing the effect of time (continuous variable) on total carbon and species as a covariate (ANCOVA, df = 28, $F_{3,23} = 0.55$, p = 0.67).

3.2. DIC and DOC released

DOC formed a greater proportion of carbon lost and recovered in seawater than DIC. After 21 d of incubation, DOC accounted for 40 ± 5% (SE) of the carbon lost from dry tissue mass compared to only 13.6 ± 2% lost as DIC; 26% of the carbon lost from tissue mass was unaccounted for using this approach (Fig. 1). Overall, DOC was released at a faster rate than DIC.

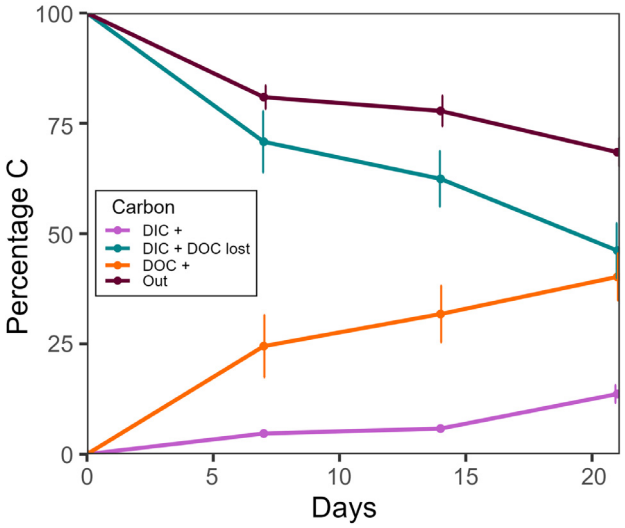

Fig. 1. Fate of carbon in anaerobic incubation experiments. Here, the carbon is calculated as a percentage of the total carbon that enters the experiment (in the form of kelp tissues). Dark purple line (Out) represents carbon leaving the kelp tissues as calculated by percentage of mass lost during incubation (23.4%). The sum of dissolved inorganic and organic carbon (DIC + DOC lost as measured in the surrounding water) does not equal the amount of carbon lost during the experiment. Approximately 26% of the mass loss in kelp fragments was unaccounted for by the carbon measured in the water

DIC increased significantly between 0 and 14 and 14 and 21 d (GLM 2, $p < 0.001$; Table 1). Differences in DIC released by different parts of kelp plants depended on the species: *Saccharina latissima* holdfasts released less DIC than those of the other 2 species, while the stipes of *Laminaria hyperborea* released more DIC than the stipes of the other species (significant material × species interaction term; Table 1; Table S3 in Section S9). Despite this significant interaction term between species and source material, DIC released from holdfasts was greater than from blade and stipe material in all 3 species (Fig. 2A, Table 1). There were no discernible differences in quantities of DIC released from blades across the 3 species.

DOC increased significantly throughout the decomposition period (Fig. 2B, Table 1: DOC for all days >0, $p < 0.001$, GLM 1). *S. latissima* released less DOC than *L. digitata* and *L. hyperborea* ($p < 0.001$, GLM 1). While the interaction term between species and tissue type was not significant, the GLM term for *L. hyperborea* stipes ($p = 0.03$, GLM 2) suggested that more DOC was released from the stipes of this species than from those of *L. digitata* and *S. latissima* (Table 1, Fig. 2).

3.3. TGA

PERMANOVA showed significant changes in the TGA derivative curves from fresh material to 21 d incubated fragments (Fig. 3). However, no significant 3-way interaction was observed in the distribution of compounds remaining after incubation among the temperature classes (Days × Tissue × Species interaction, $F_{12,119} = 1.3$, p(perm) = 0.16; Table 2). Differences in patterns among species were consistent over

Table 1. Analysis of variance after a generalised linear model (GLM) was fitted to the model showing interactions between dissolved inorganic and organic carbon (DIC and DOC, respectively) produced over time, by tissue and species. Significant ($\alpha = 0.05$) interactions are highlighted with an asterisk (*). Full GLM table of coefficients is available in Section S9, Table S3 in the Supplement, www.int-res.com/articles/suppl/m755p063_supp.pdf)

Model = mg.l ~ Days + Material × Species		df	Deviance	Resid. df	Resid. dev.	Pr(>χ^2)
Family = Gamma (link = 'log')						
Days incubated	DIC	3	11.2	132	24.2	<0.01*
Material	DIC	2	7.3	130	16.9	<0.01*
Species	DIC	2	3.2	128	13.7	<0.01*
Days incubated:Material	DIC	6	1.2	122	12.5	<0.01*
Days incubated:Species	DIC	6	0.4	116	12	0.42
Material:Species	DIC	4	3.1	112	8.9	<0.01*
Days incubated:Material:Species	DIC	10	1.9	102	7.1	<0.01*
Days incubated	DOC	3	32.9	128	67.8	<0.01*
Material	DOC	2	19.5	126	48.4	<0.01*
Species	DOC	2	14.5	124	33.9	<0.01*
Days incubated:Material	DOC	6	5.3	118	28.5	<0.01*
Days incubated:Species	DOC	5	1.9	113	26.6	0.03
Material:Species	DOC	4	0.9	109	25.7	0.24
Days incubated:Material:Species	DOC	9	7.5	100	18.2	<0.01*

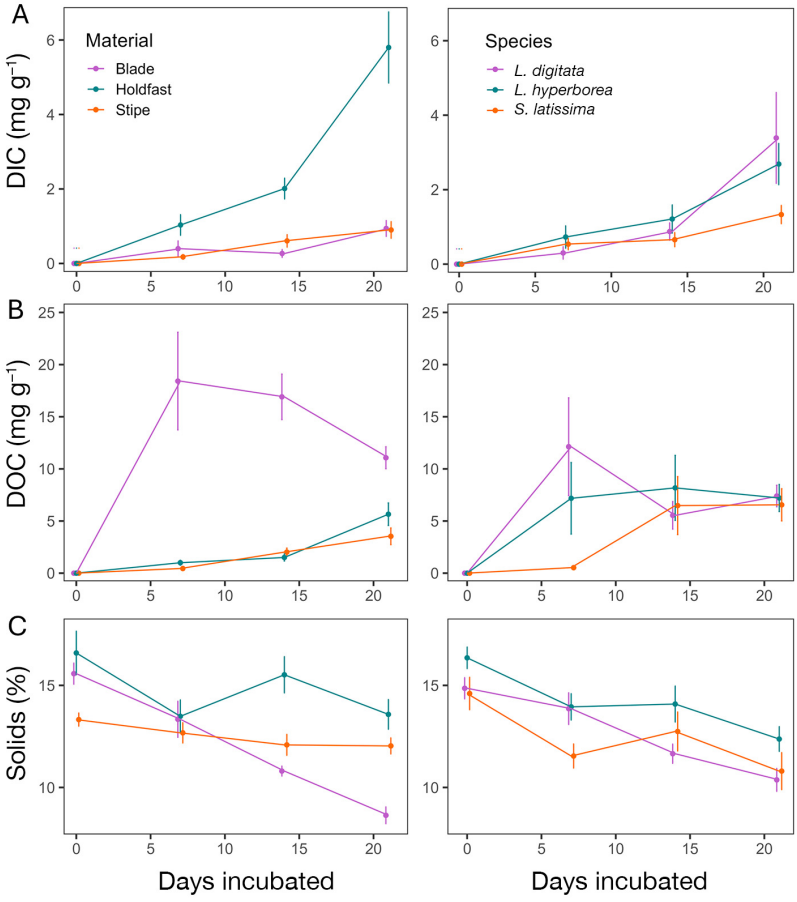

Fig. 2. Effect of time (days incubated) on (A) DIC measured in the water, (B) DOC measured in the water and (C) dry weight changes (or total solids of the material) throughout incubation for different macroalgal tissue types (left column) and different species (right column). Error bars indicate SE. Units are in mg of C produced in the water column per gram of dry weight added to the experiment

the course of the incubation (non-significant 2-way interaction between species and duration of incubation, $F_{6,119} = 1.5$, p(perm) = 0.09).

TGA curves for different plant parts (stipe, blade and holdfast) of each species changed in different ways (2-way interaction between tissue and species, $F_{4,119} = 3.1$, p(perm) = 0.002), and at different rates (2-way interaction between incubation duration and tissue tested, $F_{6,119} = 5.8$, (p(perm) = 0.001; Table 2). To investigate this 2-way interaction further, individual PERMANOVA tests were applied to each incubation stage and data were visualised as NMDS plots. The differences among TGA curves for different species and plant tissue types remained consistent from fresh fragments through to 14 d incubations (Table 3, Fig. 3). At 21 d, differences among tissues remained significant, but species differences were no longer discernible ($F_{4,35} = 1.6$, p(perm) = 0.141; Table 3). Blades had the most distinct patterns of change in TGA curves across all species, rapidly losing labile material after just 7 d of incubation (Fig. 3). Stipe material appears to retain a level of relatively labile materials (160–300°C, proteins, soluble carbohydrates and hemicellulose) throughout decomposition.

The final output from the TGA was from the standard compounds that were analysed for peak comparison. Most of the standards had a single peak which was shown in TGA, except for 2 compounds: D-mannose and phloroglucinol. Two compounds, fucoidan and cellulose, showed similar peaks of mass loss to the kelp detritus fragments (at approximately 300°C) (Fig. S3 in Section S10).

3.4. Refractory potential (Rp)

The refractory nature (Rp) of kelp detritus significantly increased (ANOVA, df = 1, $F = 30.3$, $p < 0.01$; Table 4) from 0.46 ± 0.05 (SD) to 0.50 ± 0.04 from 0 d fresh detritus to 21 d incubated fragments (Fig. 4), reflecting the leaching and consumption of labile materials that occurs during early decomposition of kelp material. There was no 3-way interaction between the effects of different tissue types, days incubated and individual species. Instead, a 2-way interaction between days incubated and species suggested that individual species retained refractory material differently over incubation periods (Table 4). *S. latissima* had a greater Rp value than the other 2 species and retained a higher Rp value after 21 d of incubation (Fig. 4).

3.5. First-order decomposition rates

First-order decomposition was calculated for blade and stipe material. The calculated half-life across 21 d of anaerobic incubations was estimated at ($t_{1/2}$) 27.8 ± 2.9 d ($k = 0.025 \pm 0.002$) for blade material and 113.2 ± 21.1 d ($k = 0.006 \pm 0.001$) for stipes (for parameters used, see Section S7 and Table S4 in Section S11). However, the biomass of holdfast material after de-

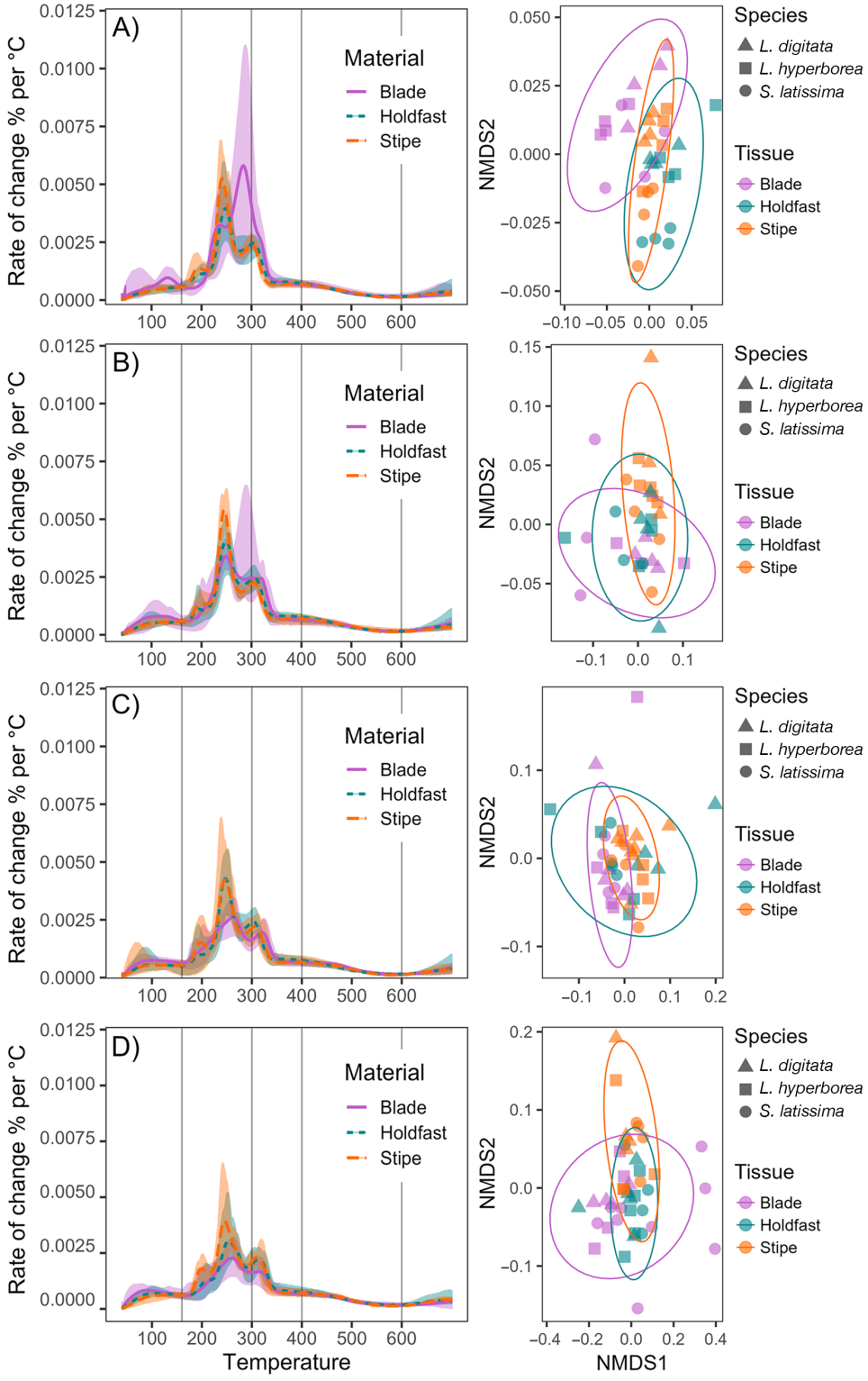

Fig. 3. Thermal degradation curves of different tissue types over the course of the incubation (left column) with dotted and dashed lines representing the means of different kelp materials and the shaded area representing the spread of data from thermogravimetric analysis (TGA). Right hand column shows the corresponding non-metric multidimensional scaling (NMDS) plots with distribution around centroids as circles (representing thallus parts). The differences observed in the refractory nature of the materials and species analysed at each incubation stage are significant except at 21 d. (A) Fresh material (0 d of incubation), (B) 7 d, (C) 14 d and (D) 21 d of anaerobic incubation

Table 2. Permutational multivariate ANOVA (PERMANOVA) of the percentage of mass lost at different temperature intervals during thermogravimetric analysis (TGA), including effects of species (Species: *Laminaria hyperborea*, *Saccharina latissima*, *L. digitata*), thallus parts (Material: stipe, holdfast, blade) and time incubated (0, 7, 14 and 21 d) (significance, set as $\alpha = 0.05$, marked with an asterisk)

Model=TI^0.5 ~ Days incubated × Material × Species, Method = 'bray'	df	*F*	R^2	Pr(>*F*)
Days incubated	3	11.14	0.14	0.001*
Material	2	4.86	0.04	0.001*
Species	2	5.22	0.04	0.001*
Days incubated:Material	6	5.77	0.14	0.001*
Days incubated:Species	6	1.51	0.04	0.096
Material:Species	4	3.14	0.05	0.002
Days incubated:Material:Species	12	1.31	0.06	0.155
Residuals	119		0.49	

Table 3. Separate PERMANOVA tests for TGA curves for decaying kelp after incubations of 0, 7, 14 and 21 d, including effects for species (Species: *Laminaria hyperborea*, *Saccharina latissima*, *L. digitata*) and thallus part types (Tissue: stipe, holdfast, blade) at each incubation stage (significance, set as $\alpha = 0.05$, marked with an asterisk)

Day	Interaction	df	*F*	R^2	Pr(>*F*)
0	Tissue	2	20.97	0.49	0.001*
0	Species	2	2.57	0.06	0.031
0	Tissue:Species	4	2.99	0.14	0.01*
0	Residuals	27		0.31	
7	Tissue	2	3.11	0.14	0.013
7	Species	2	3.36	0.15	0.012
7	Tissue:Species	4	2.14	0.19	0.029
7	Residuals	24		0.53	
14	Tissue	2	2.28	0.09	0.051
14	Species	2	3.68	0.14	0.005
14	Tissue:Species	4	2.03	0.16	0.041
14	Residuals	32		0.62	
21	Tissue	2	8.56	0.28	0.001*
21	Species	2	1.82	0.06	0.137
21	Tissue:Species	4	1.59	0.10	0.141
21	Residuals	35		0.56	

Table 4. Three-way ANOVA of the refractory potential (Rp) of kelp fragments among parts of kelps (Tissue: stipe, holdfast, blade), species (Species: *Laminaria hyperborea*, *Saccharina latissima*, *L. digitata*) and duration of incubation (0, 7, 14, 21 d). Significance, set as $\alpha = 0.05$, marked with an asterisk)

	df	*F*	Pr(>*F*)
Days.incubated	1	30.3	<0.01*
Species	2	22.2	<0.01*
Material	3	50.8	<0.01*
Days.incubated:Species	2	5.1	<0.01*
Days.incubated:Material	2	1.0	0.37
Species:Material	4	0.9	0.45
Days.incubated:Species:Material	4	1.9	0.11
Residuals	142		

composition was quite variable, and on some occasions, mass increased during incubation (this was attributed to water logging) and could not be reasonably estimated (see Fig. 2C).

4. DISCUSSION

Contrary to hypothesis (3), for 3 canopy-forming kelp species found in the North-east Atlantic, DOC was released in greater amounts than DIC over 21 d of decomposition in anaerobic conditions. Since seawater was filtered to remove anything above 20–40 µm, the DIC released in the experiment is assumed to be a product of microbial remineralisation. More DIC was released during decomposition of holdfast material than blade and stipe material. While blades released DOC at greater rates across the entire incubation period than holdfast and stipe material, incubating species separately shows that initially greater quantities of DOC came from decaying *Laminaria digitata* and *L. hyperborea* blades than from *Saccharina latissima* blades.

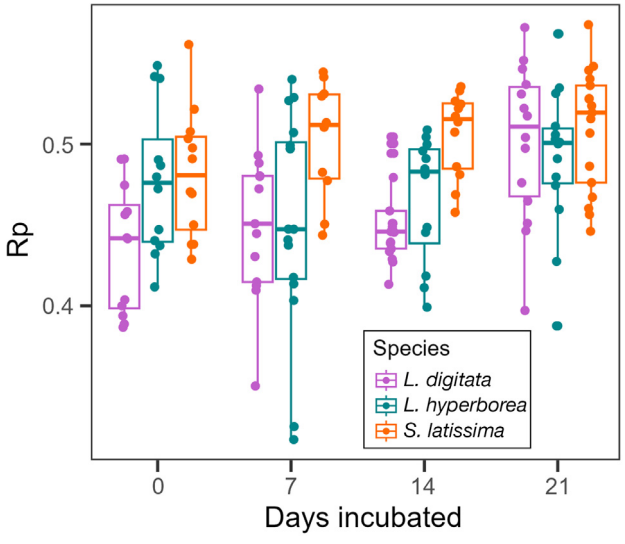

Fig. 4. Refractory potential (Rp) of macroalgal species during decomposition increases overall. Analysis of Rp data shows that *Saccharina latissima* contains the most refractory compounds and retains them the longest over decomposition stages. Standard boxplot designations apply: the minimum value at the lower whisker, the interquartile range within the box, the median (central line) and the maximum value at the upper whisker; outlier values are points beyond the whiskers

There were differences in the first-order decomposition rates of blades and stipes of the 3 species combined in anaerobic, *ex situ* experiments. A difference in decomposition rates between blades and stipes likely reflects compounds within the thallus parts ($t_{1/2}$ stipes = 113 d, blades = 28 d), but little information exists on stipe breakdown, with most studies focusing on blades because previous studies have shown they constitute almost all of the detritus leaving kelp forests (see Filbee-Dexter et al. 2018, Pessarrodona et al. 2018). Nonetheless, stipes and holdfasts are often observed in beach-cast drifts and sublittoral observations and may be significant in carbon burial given the extended breakdown time of the compounds they contain (O'Dell 2022).

In examining the aerobic decomposition of *L. hyperborea* under oxygenated (*in situ*) conditions, de Bettignies et al. (2020) showed that decomposition processes (biomass loss) started after 2 wk and 50% of biomass was lost after 8 wk of decomposition in litter bags deployed in photic conditions, in a sheltered bay. The concentration of more refractory components such as phlorotannins in degrading tissues peaked at 11 wk, and after 25 wk in the photic zone, only 16% of kelp biomass remained. Furthermore, while in the photic zone, decomposing fragments of macroalgal detritus can retain photosynthetic and reproductive function for up to 20 wk (de Bettignies et al. 2020). This continued photosynthetic activity means defensive compounds such as phlorotannins remain, which can extend the decomposition process (O'Dell 2022, Frontier et al. 2022). The dynamics are complex, but breakdown of blades in dark conditions can be faster than aerobic blade breakdown (in a situation where photosynthesis continues), with a half-life of 28 d (compared to $t_{1/2}$ = 65 d and k = 0.0107 for fresh blades of *L. hyperborea* as found by Frontier et al. 2022). This specific scenario contradicts fundamental breakdown and respiration kinetics (Middelburg 2019). As previously mentioned, the marine environment has multiple pathways and scenarios by which breakdown can occur, degradation rates appear highly sensitive to environmental conditions, and careful consideration to experimental design is important.

Other studies have shown faster aerobic decomposition rates than those of the present study. For example, the single cell thick *Ulva* sp. and the warm temperature tolerant *Gracilaria* sp. had higher k values and therefore faster decomposition rates (k = 0.34–0.51 and 0.5 respectively, $t_{1/2}$ = 1.4–2 d), as did the intertidal macroalga *Fucus vesiculosus* (k = 0.09, $t_{1/2}$ = 7.7 d), in a litter bag study conducted in the North-west Atlantic (Conover et al. 2016). Aerobic *in situ* decomposition of *Macrocystis integrifolia* had slightly faster breakdown rates than the kelps tested in the present study (k = 0.032) (Albright et al. 1980). Experiments using *in situ* litter bag decomposition have also been done in both aerobic (Filbee-Dexter et al. 2022) and anaerobic (Pedersen et al. 2021) environments. Filbee-Dexter et al. (2022) found that across a 28° latitude, the mean half-life of blade pieces was 67 d in aerobic litter bags. However, Pedersen et al. (2021) suggested that, while faster initially, anaerobic decomposition slows almost completely after 150–200 d, which can have implications for carbon storage where environmental conditions allow. There are multiple real-world scenarios under which kelp detritus might decay, and significant challenges persist in replicating these scenarios accurately. For example, litter bag experiments remove large grazers but not smaller grazers and generally happen in shallow benthic areas due to limitations of dive or snorkel teams. The conditions in the present study were designed to understand the pathways of carbon release into the water column, and to reflect the physical–chemical effect of detritus on the surrounding water. The loss of carbon by decaying kelp detritus presents a challenge to accurately re-create, and studies are not always comparable. Combined with the present study, the above results provide deeper insights into kelp decomposition, highlighting the key differences between aerobic and anaerobic processes and key differences in tissue types, which can be used in the future to inform models that will reduce the uncertainty around these dynamics.

While the results presented here reflect a detailed decomposition simulation, the tubes were sealed during decomposition, no gas escaped, and the anaerobic environment was likely created by microbial activity. In real-world scenarios, pulses of macrophytes can have a priming effect on benthic microbial communities (Trevathan-Tackett et al. 2018, Attard et al. 2023). Sealing the tubes does allow accurate measurement of gases within the seawater, but the relevance to real-world processes needs careful consideration. Most studies exploring the dynamics between aerobic and anaerobic breakdown of detritus show that the degradation rates are reduced in the absence of oxygen (Boldreel et al. 2023). The present study suggests that large detritus accumulations on the seafloor could influence oxygen concentrations in the immediate vicinity, adding further complexity to the variables that need consideration.

The complex structures of kelp holdfasts support diverse communities (Moore 1973a,b, Tuya et al. 2011,

Schaal et al. 2012, Teagle et al. 2017). Greater DIC production during decomposition from holdfasts suggests that the complexity of holdfast structure may provide greater surface area for bacteria to colonise. The slower release of DOC by holdfast and stipe material (when compared to blade material) suggests that there are more labile (easily broken down) compounds for bacteria to consume in blade tissues. The holdfasts of kelps are persistent, while the blade is continuously renewed. Therefore, microbial communities on blade material may be regenerated and variable, while those on holdfast communities persist, potentially becoming 'specialist' and adapted to the environment of the holdfast. Different parts of the macroalgal thallus do host different epibacterial and macrofaunal communities as seen for *L. digitata* (Ihua et al. 2020), *S. latissima* (Staufenberger et al. 2008) and *L. hyperborea* (Bengtsson et al. 2011). Furthermore, endophytic fungal communities have been shown to play a key role in anaerobic breakdown in some kelps (Perkins et al. 2021). An established microbial community that can tolerate benthic (low oxygen) conditions could explain the greater release of DIC by holdfasts throughout the incubation period, but does not necessarily mean that holdfasts decompose faster.

Approximately 40% of the carbon released by decaying tissue was in the form of DOC, the majority of which came from blade tissue. Similar exudation occurs in live kelp, which are net DOC producers, with maximum rates of DOC production occurring during the summer when productivity is highest (Egea et al. 2019). Large variability of within-species exudation rates has been shown (Carlson & Carlson 1984), with individuals losing between 13 and 62% of total net primary production as DOC (Reed et al. 2015). This could relate back to the variability within tissues as shown in the present study. DOC production can be up to 80% higher at mid-day compared to measurements taken at night, making light and day-length controlling factors (Abdullah & Fredriksen 2004, Hulatt et al. 2009, Maher & Eyre 2010, Reed et al. 2015). The present study tested fragments in simulated dark conditions, but light may influence production of DOC from macroalgal detritus when it persists within the photic zone. This release of dissolved compounds reflects the initial leaching phase of detritus breakdown, and has also been shown in studies of beach-cast wrack (Perkins et al. 2022). The fate of this DOC is a key unknown, but has potential to increase microbial biomass and alter the surrounding water chemistry (Barrón & Duarte 2015).

Macroalgae have been shown to contribute up to 1.5–34% of DOM pools in localised areas with turnover times estimated to be between 24 and 172 d for *Ecklonia cava* (Wada et al. 2008, Wada & Hama 2013). DOC from living macroalgal forests is also exuded at rates of up to 0.5 g C m^{-2} d^{-1} (Reed et al. 2015). DOC is significant in global carbon cycles (Jiao et al. 2010), and up to 50% of DOC produced from macroalgae (both wild and in aquaculture) is exported (Jiao et al. 2018, Gao et al. 2021, Paine et al. 2021). Significant pulses of DOC are also released from decaying beach-cast wrack at as much as 59% of the initial C content (Perkins et al. 2022). There is uncertainty surrounding the fate of this DOC, the mechanisms of release, the composition and bioavailability of the compounds and the contribution to long-term, deep-water carbon cycles (Paine et al. 2021). An aspect of DOC that is often overlooked is the component which is exuded by decomposing detritus (Lavery et al. 2013), particularly in deeper waters, where microbial breakdown is often slower (Arrieta et al. 2015). In the present study, the initial loss of DOC corresponded with the loss of a labile fraction of compounds clearly visible in the TGA assays, particularly in blade material at around 280°C (Figs. 2 & 3). However, DOC continued to be released in large amounts as the tissue parts decomposed, and thus, it is likely to play an important role in carbon cycling. A key aspect which will affect the fate of DOC is the bioavailability of the compounds within it (Wada et al. 2008, Gan et al. 2016). There are key differences in fungal and bacterial breakdown. Fungal remineralisation has been shown to significantly reduce DIC generation and increase DOC generation, suggesting that fungi play a crucial role in blue carbon cycles (Perkins et al. 2023). The compounds lost in the early peaks are within the labile temperature range, but more complex components are retained at 21 d, which will either be released as decomposition progresses or become incorporated into sediments.

TGA showed that the DOC released initially was most likely to be the labile compounds derived from blade material (the initial peaks lost at 290°C), which differs from previous studies. For example, Anastasakis et al. (2011) found that mannitol and laminarin peaked at around 340°C, alginic acid at around 220°C and fucoidan at around 200°C. These differences likely reflect the variable chemical structures of fucoidan, as the more complex structures will burn off at higher temperatures. Fucoidan may be less available than other common macroalgal sugars as a substrate for bacterial decomposition (Keith & Arnosti 2001). In the present study, pure fucoidan peaked at 309.3°C and completely com-

busted at that temperature. After 7, 14 and 21 d of decomposition, all TGA profiles retained a peak at this temperature, suggesting that fucoidan remains within holdfast and stipe tissues through to later stages of decomposition. Future studies could look in detail at the specific polysaccharide content of DOC and the refractory nature of compounds released to test this theory.

S. latissima had a higher Rp value than *L. digitata* and *L. hyperborea* throughout incubations, and retained DOC for longer. This species is adapted to more turbid, sheltered areas and is common in fjords (Gevaert et al. 2001, Borum et al. 2002, Burrows et al. 2014). Fjords are areas where the accumulation of organic carbon in sediments is significantly higher than further from shore (Smith et al. 2015, Smeaton et al. 2020). Slower decomposition can have implications for carbon storage in sediments, potentially allowing burial or further transport of detritus before complete degradation occurs. This will be especially common in accumulations of macroalgal detritus within fjords which persist for some time (i.e. greater than 24 h) and have been shown to induce anoxia (Attard et al. 2023). Since *S. latissima* is an abundant species in upper (more sheltered) fjord regions, the findings here suggest it plays an important role in carbon turnover and storage in these areas.

The general Rp values from kelp species tested here are higher than those of some terrestrial plants (e.g. barley straw: 0.17–0.37) and higher than plants rich in structural carbohydrates (around 0.3; Kristensen 1990) in Scottish sea lochs. The analysis of 475 Scottish fjord samples by Smeaton & Austin (2022) found the sediment Rp ranged from 0.32 to 0.89 (mean 0.64). Loh et al. (2002) found that Rp values ranged from 0.3 to 0.62 in sediments from the head to the mouth (open sea area) of Loch Creran and Loch Etive, suggesting that sediments might be more influenced by kelp detritus further from fluvial/terrestrial input.

Methane (CH_4) production was not measured in this experiment and is a key process in anaerobic decomposition (McKennedy & Sherlock 2015). In anaerobic experiments, *L. digitata* and *L. hyperborea* produced between 80 and 184 l of CH_4 kg^{-1} d^{-1}, when digesters were fed continuously and depending on the volatile state of the feed stock (Hanssen et al. 1987, Kerner et al. 1991). Large brown seaweeds, such as *S. latissima,* have been shown to produce 1.5–2.8 times more CH_4 than other species (e.g. green and red algae) in anaerobic digestion (Nielsen & Heiske 2011). Therefore, there was a portion of carbon produced in this experiment that was not measured, in the form of CH_4. This may explain the approximately 26% of carbon that remained unaccounted for at the end of the experiment across all tissues and species. Anoxic carbon remineralisation is generally dominated by sulphate reduction, and macroalgal detritus is rich in available sulphates. In the water column, the result is the production of hydrogen sulphide (H_2S) (Glud et al. 2004, Boldreel et al. 2023). Neither H_2S nor CH_4 was measured here, but both require careful consideration. Thus, future studies should incorporate H_2S and CH_4 measurement protocols and investigate H_2S-producing microbes and their inhibitory capacity on CH_4 production (Jung et al. 2013, 2019).

5. CONCLUSIONS

This study provides valuable insights into the dynamics surrounding anaerobic decomposition of 3 stipitate kelps from the North-east Atlantic. The differences in DIC and DOC release during decomposition are highlighted, with a considerable amount of DOC released in the initial stages of decomposition. After 21 d of decomposition, approximately 40% of the carbon added to the experiments was released in DOC form. The fate of this DOC is uncertain, but there are implications for contribution to larger, global carbon cycles. The degradation rates of these kelp species are lower than those of other macroalgae species previously tested (Albright et al. 1980, Conover et al. 2016, de Bettignies et al. 2020), which again can have implications for carbon storage in sediments on the coastal shelf and in fjords in the North-east Atlantic. *Saccharina latissima* is highlighted as showing different degradation dynamics and greater refractory potential (Rp) than the *Laminaria* species tested here, and is potentially a key contributor to blue carbon burial in fjord systems. Estimates of Rp indicate that kelps are not as labile as previously suggested, and although kelps are carbohydrate rich and lack structural components such as lignin, they may contain other compounds that slow decomposition. These compounds are retained through decomposition, making tissues less labile as they age, thus increasing the potential for burial and contribution to blue carbon storage.

Data availability. The data presented in the study are deposited in the figshare repository 'Anaerobic decomposition dynamics of three important stipitate kelps in the North-east Atlantic. With implications for blue carbon storage' (https://figshare.com/projects/Anaerobic_decomposition_dynamics_of_three_important_stipitate_kelps_in_the_Northeast_Atlantic_With_Implications_for_blue_carbon_storage/167525):

O'Dell, A. (2023). Calculating k. doi:10.6084/m9.figshare.22895180.v1.
O'Dell, A. (2023). Temperature Intervals. doi:10.6084/m9.figshare.22895084.v1.
O'Dell, A. (2023). DIC and DOC data. doi:10.6084/m9.figshare.22894211.v1.
O'Dell, A. (2023). TGA files. doi:10.6084/m9.figshare.22894082.v1.

Acknowledgements. This work was conducted at the Scottish Association for Marine Science (SAMS) funded in part by the Scottish Blue Carbon Forum (SBCF), Scottish Government Marine Directorate and the University of the Highlands and Islands and forms part of A.R.O'D.'s PhD thesis. D.A.S. was funded by a UKRI Future Leaders Fellowship (MR/S032827/1). A.R.O'D. thanks Dr. Natalie Hicks for help with the experimental design; Dr. Tim Brand and Dr. Sharon McNeil for assistance in the lab; and all authors for their contributions. A.R.O'D. also thanks the University of St Andrews for access to laboratory facilities for TGA.

LITERATURE CITED

Abdullah MI, Fredriksen S (2004) Production, respiration and exudation of dissolved organic matter by the kelp *Laminaria hyperborea* along the west coast of Norway. J Mar Biol Assoc UK 84:887–894

Albright LJ, Chocair J, Masuda K, Valdes M (1980) *In situ* degradation of the kelps *Macrocystis integrifolia* and *Nereocystis luetkeana* in British Columbia coastal waters. Nat Can 107:3–10

Anastasakis K, Ross AB, Jones JM (2011) Pyrolysis behaviour of the main carbohydrates of brown macro-algae. Fuel 90:598–607

Arrieta JM, Mayol E, Hansman RL, Herndl GJ, Dittmar T, Duarte CM (2015) Dilution limits dissolved organic carbon utilization in the deep ocean. Science 348:331–333

Attard KM, Lyssenko A, Rodil IF (2023) High metabolism and periodic hypoxia associated with drifting macrophyte detritus in the shallow subtidal Baltic Sea. Biogeosciences 20:1713–1724

Barrón C, Duarte CM (2015) Dissolved organic carbon pools and export from the coastal ocean. Global Biogeochem Cycles 29:1725–1738

Bengtsson MM, Sjøtun K, Storesund JE, Øvreås L (2011) Utilization of kelp-derived carbon sources by kelp surface-associated bacteria. Aquat Microb Ecol 62:191–199

Bockmon EE, Dickson AG (2015) An inter-laboratory comparison assessing the quality of seawater carbon dioxide measurements. Mar Chem 171:36–43

Boldreel EH, Attard KM, Hancke K, Glud RN (2023) Microbial degradation dynamics of farmed kelp deposits from *Saccharina latissima* and *Alaria esculenta*. Mar Ecol Prog Ser 709:1–15

Borum J, Pedersen M, Krause-Jensen D, Christensen P, Nielsen K (2002) Biomass, photosynthesis and growth of *Laminaria saccharina* in a high-arctic fjord, NE Greenland. Mar Biol 141:11–19

Burrows MT, Smale D, O'Connor N, Rein HV, Moore P (2014) Marine Strategy Framework Directive indicators for UK kelp habitats. 1. Developing proposals for potential indicators. SAMS/MBA/QUB/UAber for JNCC, Peterborough

Burton RA, Gidley MJ, Fincher GB (2010) Heterogeneity in the chemistry, structure and function of plant cell walls. Nat Chem Biol 6:724–732

Carlson DJ, Carlson ML (1984) Reassessment of exudation by fucoid macroalgae. Limnol Oceanogr 29:1077–1087

Conover J, Green LA, Thornber CS (2016) Biomass decay rates and tissue nutrient loss in bloom and non-bloom-forming macroalgal species. Estuar Coast Shelf Sci 178:58–64

Dafner EV, Wangersky PJ (2002) A brief overview of modern directions in marine DOC studies. II. Recent progress in marine DOC studies. J Environ Monit 4:55–69

Davidson K, Gilpin LC, Pete R, Brennan D, McNeill S, Moschonas G, Sharples J (2013) Phytoplankton and bacterial distribution and productivity on and around Jones Bank in the Celtic Sea. Prog Oceanogr 117:48–63

de Bettignies F, Dauby P, Thomas F, Gobet A and others (2020) Degradation dynamics and processes associated with the accumulation of *Laminaria hyperborea* (Phaeophyceae) kelp fragments: an in situ experimental approach. J Phycol 56:1481–1492

Deniaud-Bouët E, Hardouin K, Potin P, Kloareg B, Hervé C (2017) A review about brown algal cell walls and fucose-containing sulfated polysaccharides: cell wall context, biomedical properties and key research challenges. Carbohydr Polym 175:395–408

Dickson AG (2019) Certificate of analysis: reference material for oceanic CO_2 measurements. Batch 186 (bottled June 28, 2019). Scripps Institution of Oceanography, La Jolla, CA. https://www.ncei.noaa.gov/access/ocean-carbon-acidification-data-system/oceans/Dickson_CRM/rmdata/Batch186.pdf

Dickson AG, Sabine CL, Christian JR, Bargeron CP (eds) (2007) Guide to best practices for ocean CO_2 measurements. North Pacific Marine Science Organization, Sidney

Egea LG, Barrón C, Jiménez–Ramos R, Hernández I, Vergara JJ, Pérez–Lloréns JL, Brun FG (2019) Coupling carbon metabolism and dissolved organic carbon fluxes in benthic and pelagic coastal communities. Estuar Coast Shelf Sci 227:106336

Ehrnsten E, Norkko A, Timmermann K, Gustafsson BG (2019) Benthic-pelagic coupling in coastal seas — modelling macrofaunal biomass and carbon processing in response to organic matter supply. J Mar Syst 196:36–47

Enríquez S, Duarte CM, Sand-Jensen K (1993) Patterns in decomposition rates among photosynthetic organisms: the importance of detritus C:N:P content. Oecologia 94:457–471

Filbee-Dexter K, Wernberg T (2020) Substantial blue carbon in overlooked Australian kelp forests. Sci Rep 10:12341

Filbee-Dexter K, Wernberg T, Norderhaug KM, Ramirez-Llodra E, Pedersen MF (2018) Movement of pulsed resource subsidies from kelp forests to deep fjords. Oecologia 187:291–304

Filbee-Dexter K, Feehan C, Smale D, Krumhansl K and others (2022) Kelp carbon sink potential decreases with warming due to accelerating decomposition. PLOS Biol 20(8):e3001702

Filbee-Dexter K, Pessarrodona A, Pedersen MF, Wernberg T and others (2024) Carbon export from seaweed forests to deep ocean sinks. Nat Geosci 17:552–558

Frontier N, Mulas M, Foggo A, Smale DA (2022) The influence of light and temperature on detritus degradation rates for kelp species with contrasting thermal affinities. Mar Environ Res 173:105529

Gan S, Wu Y, Zhang J (2016) Bioavailability of dissolved organic carbon linked with the regional carbon cycle in the East China Sea. Deep Sea Res II 124:19–28

Gao Y, Zhang Y, Du M, Lin F and others (2021) Dissolved organic carbon from cultured kelp *Saccharina japonica*: production, bioavailability, and bacterial degradation rates. Aquacult Environ Interact 13:101–110

Gevaert F, Davoult D, Creach A, Kling R, Janquin MA, Seuront L, Lemoine Y (2001) Carbon and nitrogen content of *Laminaria saccharina* in the eastern English Channel: biometrics and seasonal variations. J Mar Biol Assoc UK 81:727

Gholz HL, Wedin DA, Smitherman SM, Harmon ME, Parton WJ (2000) Long-term dynamics of pine and hardwood litter in contrasting environments: toward a global model of decomposition. Glob Change Biol 6:751–765

Gilson AR, Smale DA, Burrows MT, O'Connor NE (2021) Spatio-temporal variability in the deposition of beach-cast kelp (wrack) and inter-specific differences in degradation rates. Mar Ecol Prog Ser 674:89–102

Glud RN, Rysgaard S, Fenchel T, Nielsen PH (2004) A conspicuous H_2S-oxidizing microbial mat from a high-latitude Arctic fjord (Young Sound, NE Greenland). Mar Biol 145:51–60

Goyet C, Snover AK (1993) High-accuracy measurements of total dissolved inorganic carbon in the ocean: comparison of alternate detection methods. Mar Chem 44: 235–242

Green-Cavrielidis LA, MacKechnie F, Thornber CS, Gomez-Chiarri M (2018) Bloom-forming macroalgae (*Ulva* spp.) inhibit the growth of co-occurring macroalgae and decrease eastern oyster larval survival. Mar Ecol Prog Ser 595:27–37

Haavisto F, Koivikko R, Jormalainen V (2017) Defensive role of macroalgal phlorotannins: benefits and trade-offs under natural herbivory. Mar Ecol Prog Ser 566:79–90

Hanssen JF, Indergaard M, Østgaard K, Bævre OA, Pedersen TA, Jensen A (1987) Anaerobic digestion of *Laminaria* spp. and *Ascophyllum nodosum* and application of end products. Biomass 14:1–13

Hori M, Bayne CJ, Kuwae T (2019) Blue carbon: characteristics of the ocean's sequestration and storage ability of carbon dioxide. In: Kuwae T, Hori M (eds) Blue carbon in shallow coastal ecosystems: carbon dynamics, policy, and implementation. Springer, Singapore, p 1–31

Hulatt CJ, Thomas DN, Bowers DG, Norman L, Zhang C (2009) Exudation and decomposition of chromophoric dissolved organic matter (CDOM) from some temperate macroalgae. Estuar Coast Shelf Sci 84:147–153

Ihua MW, FitzGerald JA, Guihéneuf F, Jackson SA, Claesson MJ, Stengel DB, Dobson ADW (2020) Diversity of bacteria populations associated with different thallus regions of the brown alga *Laminaria digitata*. PLOS ONE 15:e0242675

Jiao N, Herndl GJ, Hansell DA, Benner R and others (2010) Microbial production of recalcitrant dissolved organic matter: long-term carbon storage in the global ocean. Nat Rev Microbiol 8:593–599

Jiao N, Liang Y, Zhang Y, Liu J and others (2018) Carbon pools and fluxes in the China Seas and adjacent oceans. Sci China Earth Sci 61:1535–1563

Johnson A, Koehl M (1994) Maintenance of dynamic strain similarity and environmental stress factor in different flow habitats: thallus allometry and material properties of a giant kelp. J Exp Biol 195:381–410

Jung KA, Lim SR, Kim Y, Park JM (2013) Potentials of macroalgae as feedstocks for biorefinery. Bioresour Technol 135:182–190

Jung H, Kim J, Lee C (2019) Temperature effects on methanogenesis and sulfidogenesis during anaerobic digestion of sulfur-rich macroalgal biomass in sequencing batch reactors. Microorganisms 7:682

Keith SC, Arnosti C (2001) Extracellular enzyme activity in a river-bay-shelf transect: variations in polysaccharide hydrolysis rates with substrate and size class. Aquat Microb Ecol 24:243–253

Kerner KN, Hanssen JF, Pedersen TA (1991) Anaerobic digestion of waste sludges from the alginate extraction process. Bioresour Technol 37:17–24

Kerrison PD, Stanley MS, Smet DD, Buyle G, Hughes AD (2019) Holding (not so) fast: surface chemistry constrains kelp bioadhesion. Eur J Phycol 54:291–299

Krause-Jensen D, Duarte CM (2016) Substantial role of macroalgae in marine carbon sequestration. Nat Geosci 9:737–742

Krause-Jensen D, Lavery P, Serrano O, Marbà N, Masque P, Duarte CM (2018) Sequestration of macroalgal carbon: the elephant in the Blue Carbon room. Biol Lett 14:20180236

Kristensen E (1990) Characterization of biogenic organic matter by stepwise thermogravimetry (STG). Biogeochemistry 9:135–159

Krumhansl KA, Scheibling RE (2011) Detrital production in Nova Scotian kelp beds: patterns and processes. Mar Ecol Prog Ser 421:67–82

Krumhansl KA, Scheibling RE (2012) Production and fate of kelp detritus. Mar Ecol Prog Ser 467:281–302

Laliberté E, Adair EC, Hobbie SE (2012) Estimating litter decomposition rate in single-pool models using nonlinear beta regression. PLOS ONE 7:e45140

Lavery PS, McMahon K, Weyers J, Boyce MC, Oldham CE (2013) Release of dissolved organic carbon from seagrass wrack and its implications for trophic connectivity. Mar Ecol Prog Ser 494:121–133

Loh PS, Reeves AD, Overnell J, Harvey SM, Miller AEJ (2002) Assessment of terrigenous organic carbon input to the total organic carbon in sediments from Scottish transitional waters (sea lochs): methodology and preliminary results. Hydrol Earth Syst Sci 6:959–970

Macreadie PI, Nielsen DA, Kelleway JJ, Atwood TB and others (2017) Can we manage coastal ecosystems to sequester more blue carbon? Front Ecol Environ 15:206–213

Macreadie PI, Anton A, Raven JA, Beaumont N and others (2019) The future of Blue Carbon science. Nat Commun 10:3998

Maher DT, Eyre BD (2010) Benthic fluxes of dissolved organic carbon in three temperate Australian estuaries: implications for global estimates of benthic DOC fluxes. J Geophys Res Biogeosci 115:G04039

McKennedy J, Sherlock O (2015) Anaerobic digestion of marine macroalgae: a review. Renew Sustain Energy Rev 52:1781–1790

Mcleod E, Chmura GL, Bouillon S, Salm R and others (2011) A blueprint for blue carbon: toward an improved understanding of the role of vegetated coastal habitats in sequestering CO_2. Front Ecol Environ 9:552–560

Meentemeyer V (1978) Macroclimate and lignin control of litter decomposition rates. Ecology 59:465–472

Middelburg JJ (2019) Marine carbon biogeochemistry. Springer, Berlin

Mills DB, Francis WR, Vargas S, Larsen M, Elemans CP, Canfield DE, Wörheide G (2018) The last common ancestor of animals lacked the HIF pathway and respired in low-oxygen environments. ELife 7:e31176

Moore PG (1973a) The kelp fauna of northeast Britain. I. Introduction and the physical environment. J Exp Mar Biol Ecol 13:97–125

Moore PG (1973b) The larger Crustacea associated with holdfasts of kelp (*Laminaria hyperborea*) in North-East Britain. Cah Biol Mar 14:493–518

Nielsen HB, Heiske S (2011) Anaerobic digestion of macroalgae: methane potentials, pre-treatment, inhibition and co-digestion. Water Sci Technol 64:1723–1729

O'Dell A (2022) Scotland's Blue Carbon: the contribution from seaweed detritus. PhD thesis, University of the Highlands and Islands, Scottish Association for Marine Science, Oban

Oksanen J, Blanchet FG, Kindt R, Legendre P and others (2020) Vegan: community ecology package, version 2.6. https://cran.r-project.org/web/packages/vegan/index.html

Ola A, Lovelock CE (2021) Decomposition of mangrove roots depends on the bulk density they grew in. Plant Soil 460: 177–187

Olson JS (1963) Energy storage and the balance of producers and decomposers in ecological systems. Ecology 44: 322–331

Ortega A, Geraldi NR, Alam I, Kamau AA and others (2019) Important contribution of macroalgae to oceanic carbon sequestration. Nat Geosci 12:748–754

Paine ER, Schmid M, Boyd PW, Diaz-Pulido G, Hurd CL (2021) Rate and fate of dissolved organic carbon release by seaweeds: a missing link in the coastal ocean carbon cycle. J Phycol 57:1375–1391

Pedersen MF, Filbee-Dexter K, Frisk NL, Sárossy Z, Wernberg T (2021) Carbon sequestration potential increased by incomplete anaerobic decomposition of kelp detritus. Mar Ecol Prog Ser 660:53–67

Pendleton L, Donato DC, Murray BC, Crooks S and others (2012) Estimating global 'blue carbon' emissions from conversion and degradation of vegetated coastal ecosystems. PLOS ONE 7:e43542

Perkins AK, Rose AL, Grossart HP, Rojas-Jimenez K, Barroso Prescott SK, Oakes JM (2021) Oxic and anoxic organic polymer degradation potential of endophytic fungi from the marine macroalga, *Ecklonia radiata*. Front Microbiol 12:726138

Perkins AK, Santos IR, Rose AL, Schulz KG and others (2022) Production of dissolved carbon and alkalinity during macroalgal wrack degradation on beaches: a mesocosm experiment with implications for blue carbon. Biogeochemistry 160:159–175

Perkins AK, Rose AL, Grossart HP, Schulz KG and others (2023) Fungi increases kelp (*Ecklonia radiata*) remineralisation and dissolved organic carbon, alkalinity, and dimethylsulfoniopropionate (DMSP) production. Sci Total Environ 905:166957

Pessarrodona A, Moore PJ, Sayer MDJ, Smale DA (2018) Carbon assimilation and transfer through kelp forests in the NE Atlantic is diminished under a warmer ocean climate. Glob Change Biol 24:4386–4398

Prescott CE, Zabek LM, Staley CL, Kabzems R (2000) Decomposition of broadleaf and needle litter in forests of British Columbia: influences of litter type, forest type, and litter mixtures. Can J Res 30:1742–1750

Queirós AM, Stephens N, Widdicombe S, Tait K and others (2019) Connected macroalgal-sediment systems: blue carbon and food webs in the deep coastal ocean. Ecol Monogr 89:e01366

R Core Team (2022) R: a language and environment for statistical computing. R Foundation for Statistical Computing, Vienna

Reed DC, Carlson CA, Halewood ER, Nelson JC, Harrer SL, Rassweiler A, Miller RJ (2015) Patterns and controls of reef-scale production of dissolved organic carbon by giant kelp *Macrocystis pyrifera*. Limnol Oceanogr 60:1996–2008

Schaal G, Riera P, Leroux C (2012) Food web structure within kelp holdfasts (*Laminaria*): a stable isotope study. Mar Ecol 33:370–376

Schiener P, Black KD, Stanley MS, Green DH (2015) The seasonal variation in the chemical composition of the kelp species *Laminaria digitata, Laminaria hyperborea, Saccharina latissima,* and *Alaria esculenta*. J Appl Phycol 27: 363–373

Smale DA, Pessarrodona A, King N, Moore PJ (2022) Examining the production, export, and immediate fate of kelp detritus on open-coast subtidal reefs in the Northeast Atlantic. Limnol Oceanogr 67:S36–S49

Smeaton C, Austin WEN (2019) Where's the carbon: exploring the spatial heterogeneity of sedimentary carbon in mid-latitude fjords. Front Earth Sci 7:269

Smeaton C, Austin WEN (2022) Quality not quantity: prioritizing the management of sedimentary organic matter across continental shelf seas. Geophys Res Lett 49: e2021GL097481

Smeaton C, Austin W, Turrell WR (2020) Re-evaluating Scotland's sedimentary carbon stocks. Scott Mar Freshw Sci 11:1–16

Smith RW, Bianchi TS, Allison M, Savage C, Galy V (2015) High rates of organic carbon burial in fjord sediments globally. Nat Geosci 8:450–453

Staufenberger T, Thiel V, Wiese J, Imhoff JF (2008) Phylogenetic analysis of bacteria associated with *Laminaria saccharina*. FEMS Microbiol Ecol 64:65–77

Teagle H, Hawkins SJ, Moore PJ, Smale DA (2017) The role of kelp species as biogenic habitat formers in coastal marine ecosystems. J Exp Mar Biol Ecol 492:81–98

Trevathan-Tackett SM, Kelleway J, Macreadie PI, Beardall J, Ralph P, Bellgrove A (2015) Comparison of marine macrophytes for their contributions to blue carbon sequestration. Ecology 96:3043–3057

Trevathan-Tackett SM, Thomson ACG, Ralph PJ, Macreadie PI (2018) Fresh carbon inputs to seagrass sediments induce variable microbial priming responses. Sci Total Environ 621:663–669

Tuya F, Larsen K, Platt V (2011) Patterns of abundance and assemblage structure of epifauna inhabiting two morphologically different kelp holdfasts. Hydrobiologia 658: 373–382

Vetter EW, Dayton PK (1999) Organic enrichment by macrophyte detritus, and abundance patterns of megafaunal populations in submarine canyons. Mar Ecol Prog Ser 186:137–148

Wada S, Hama T (2013) The contribution of macroalgae to the coastal dissolved organic matter pool. Estuar Coast Shelf Sci 129:77–85

Wada S, Aoki MN, Mikami A, Komatsu T and others (2008) Bioavailability of macroalgal dissolved organic matter in seawater. Mar Ecol Prog Ser 370:33–44

Walker FT (1954) Distribution of Laminariaceae around Scotland. Nature 173:766–768

Zhang D, Hui D, Luo Y, Zhou G (2008) Rates of litter decomposition in terrestrial ecosystems: global patterns and controlling factors. J Plant Ecol 1:85–93

Editorial responsibility: Robinson Fulweiler, Boston, Massachusetts, USA
Reviewed by: K. Hancke, R. Forster and 1 anonymous referee

Submitted: May 31, 2024
Accepted: January 8, 2025
Proofs received from author(s): February 21, 2025